# Fission fragment mass distributions in $^{35}$Cl + $^{144,154}$Sm reactions

R. Tripathi,[1,*] S. Sodaye,[1] K. Sudarshan,[1] B. K. Nayak,[2] A. Jhingan,[3] P. K. Pujari,[1] K. Mahata,[2] S. Santra,[2] A. Saxena,[2] E. T. Mirgule,[2] and R. G. Thomas[2]

[1]*Radiochemistry Division, Bhabha Atomic Research Centre, Mumbai-400085, India*

[2]*Nuclear Physics Division, Bhabha Atomic Research Centre, Mumbai-400085, India*

[3]*Inter University Accelerator Centre, Aruna Asaf Ali Marg, New Delhi-110067, India*

(Received 24 June 2015; published 12 August 2015)

**Background:** A new type of asymmetric fission was observed in $\beta$-delayed fission of $^{180}$Tl [Phys. Rev. Lett. **105**, 252502 (2010)] as symmetric mass distribution would be expected based on conventional shell effects leading to the formation of $N = 50$ fragments. Following this observation, theoretical calculations were carried out which predict asymmetric mass distribution for several mercury isotopes around mass region of ∼180 at low and moderate excitation energies [Moller, Randrup, and Sierk, Phys. Rev. C **85**, 024306 (2012); Andreev, Adamian, and Antonenko, *ibid.* **86**, 044315 (2012)]. Studies on fission fragment mass distribution are required in this mass region to investigate this newly observed phenomenon.

**Purpose:** The fission fragment mass distributions have been measured in $^{35}$Cl + $^{144,154}$Sm reactions at $E_{\rm lab}$ = 152.5, 156.1, and 163.7 MeV populating compound nuclei in the mass region of ∼180 with variable excitation energy and neutron number to investigate the nature of mass distribution.

**Method:** The fission fragment mass distribution has been obtained by measuring the "time of flight (TOF)" of fragments with respect to the beam pulse using two multiwire proportional counters placed at $\theta_{\rm lab} = \pm 65.5^{\circ}$ with respect to the beam direction. From the TOF of fragments, their velocities were determined, which were used to obtain mass distribution taking the compound nucleus as the fissioning system.

**Results:** For both systems, mass distributions, although, appear to be symmetric, could not be fitted well by a single Gaussian. The deviation from a single Gaussian fit is more pronounced for the $^{35}$Cl + $^{144}$Sm reaction. A clear flat top mass distribution has been observed for the $^{35}$Cl + $^{144}$Sm reaction at the lowest beam energy. The mass distribution is very similar to that observed in the $^{40}$Ca + $^{142}$Nd reaction, which populated a similar compound nucleus, but for the pronounced dip in the symmetric region [Phys. Rev. C **91**, 064605 (2015)].

**Conclusions:** The present study shows that the mass distribution deviates from that expected on the basis of a pure liquid drop model in the mass region of ∼180, indicating a contribution from asymmetric fission. The contribution from asymmetric fission is more pronounced for the $^{35}$Cl + $^{144}$Sm reaction as evident from the large deviation of the fission fragment mass distribution from the single Gaussian fit. This is consistent with the observation of an asymmetric component in the $^{40}$Ca + $^{142}$Nd reaction in a recent study [Phys. Rev. C **91**, 064605 (2015)]. The contribution from asymmetric component is also consistent with the theoretical predictions by Moller *et al.* [Phys. Rev. C **85**, 024306 (2012)], although the magnitude of the effect appears to be smaller.

DOI: 10.1103/PhysRevC.92.024610 PACS number(s): 25.70.Jj, 25.85.Ge

## I. INTRODUCTION

The fragment mass distribution has been an important fission observable which provided information about the potential-energy landscape of the fissioning nucleus. The potential energy of the fissioning nucleus starting from the equilibrium configuration to the scission point is described by a liquid drop model (LDM) [1], which can explain the origin of the fission barrier arising from the opposite trends of Coulomb and surface energies during deformation. In the liquid drop model, the saddle and the scission points are identified as key stages in the fission process. Both saddle-point [2] and scission-point models [3] have been proposed to explain the mass distribution in terms of the potential energy of the fissioning system at saddle and scission points, respectively. Although the LDM qualitatively explained the fission process, it failed to explain the asymmetric nature of fission fragment mass distribution in low-energy fission of actinides, which could be explained after incorporation of shell and pairing corrections to the LDM potential energy [4]. Thus, the LDM combined with single-particle effects could explain fission fragment mass distribution over a wide range of excitation energy and fissioning systems. Shell effects have also been reported to result in asymmetric components in mass distribution in heavy-ion-induced fission, owing to the entrance channel dynamics [5–8].

Recently, in a study of $\beta$-delayed fission of $^{180}$Tl at ISOLDE, CERN, a new type of asymmetric fission was observed [9], resulting in the peaking of mass distribution at $A_{\rm L} \sim 80$ and $A_{\rm H} \sim 100$, where $A_{\rm L}$ and $A_{\rm H}$ are light and heavy fragment masses, respectively [9]. This observation was different from that expected on the basis of conventional shell effects, which would predict symmetric fission due to the $N = 50$ shell closure in the fragments. Observation of asymmetric mass distribution was attributed to the localized single-particle effects in the vicinity of the saddle point [9,10]. Moller *et al.* [10] carried out a detailed calculation for various mercury isotopes in the mass region around ∼180. Based on these calculations, asymmetric mass distribution is predicted

*Corresponding author: rahult@barc.gov.in

 

TABLE I. Details of beam energy ($E_{lab}$), excitation energy ($E^*_{CN}$) of the compound nucleus, average excitation energy of the fissioning nucleus ($\langle E^*_f \rangle$), and prefission neutrons ($\nu_{pre}$) for $^{35}Cl + ^{144,154}Sm$ reactions. $\langle E^*_f \rangle$ and $\nu_{pre}$ values were calculated using the code PACE2 [15].

| $E_{lab}$(MeV) | $^{35}Cl + ^{144}Sm$ | | $^{35}Cl + ^{154}Sm$ | |
|---|---|---|---|---|
| | $E^*_{CN}(\langle E^*_f \rangle)$ (MeV) | $\nu_{pre}$ | $E^*_{CN}(\langle E^*_f \rangle)$ (MeV) | $\nu_{pre}$ |
| 152.5 | 36.7 (29.0) | 0.66 | 56.4 (44.4) | 1.18 |
| 156.1 | 39.6 (30.6) | 0.77 | 59.3 (44.2) | 1.37 |
| 163.7 | 45.7 (35.3) | 0.82 | 65.5 (38.2) | 2.52 |

for many mercury isotopes up to excitation energy as high as 40 MeV. In another calculation, Andreev *et al.* [11] showed that the observed asymmetric mass distribution can be understood in terms of conventional fragment shell effects at the scission point. In these calculations, observation of most probable mass split away from symmetry has been attributed to the deformed scission-point configuration. These calculations predict asymmetric mass distribution even at much higher excitation energies. These recent experimental and theoretical observations warrant more experimental measurements on fission fragment mass distribution in the mass region of ∼180 with variable excitation energy of the fissioning nucleus. The heavy-ion fusion-fission process is suitable for this purpose where it is possible to populate different fissioning systems with variable excitation energies. In a recent study of fission fragment mass distribution in $^{12}C + ^{180}W$ and $^{40}Ca + ^{142}Nd$ reactions, an asymmetric component was observed in the latter reaction [12].

In the present paper, mass distributions have been measured in the $^{35}Cl + ^{144,154}Sm$ reaction at $E_{lab} =$ 152.5, 156.1, and 163.7 MeV. The two reactions populate fissioning systems with widely different neutron numbers. Due to the magic neutron number for $^{144}Sm$, the $Q_{gg}$ value for compound nucleus formation is highly negative leading to low excitation energy of the compound nucleus. Compound nucleus excitation energies for the two reactions are given in Table I. Data from the present measurement have been compared with that from Ref. [12].

## II. EXPERIMENTAL DETAILS AND DATA ANALYSIS

Experiments were carried out at BARC-TIFR Pelletron LINAC facility, Mumbai. Targets of $^{144}Sm$ (93.8%) and $^{154}Sm$ (>99%) with thicknesses of ∼120 $\mu g/cm^2$, electrodeposited on Al backing of thicknesses of 550 $\mu g/cm^2$, were bombarded with a $^{35}Cl$ beam with the Al layer facing the beam. Beam energies given in the Table I are the energies in the target after energy degradation in the backing foil. Two multiwire proportional counters (MWPCs) were placed around the folding angle ($\theta_{lab} = \pm 65.5^\circ$) for a coincidence measurement of the fission fragments recoiling out of the target. The size of each MWPC was 12.6 × 7.6 $cm^2$. Signals of MWPCs were recorded in a time-to-digital converter triggered with the rf signal corresponding to the beam pulse (width ∼1 ns).

A plot of timing spectrum ($T_1$ vs $T_2$; subscripts 1 and 2 refer to the fragments detected in detector 1; $\phi = 87.5^\circ$ and 2; $\phi = 272.5^\circ$, respectively) for the $^{35}Cl + ^{144}Sm$ reaction at $E_{lab} = 156.1$ MeV is shown in Fig. 1(a). Due to the limited angular coverage of the detector, events were selected within a narrow range of center-of-mass (c.m.) angle ($\theta_{cm}$) from 82° to 99° for $^{35}Cl + ^{144}Sm$ and 83° to 100° for $^{35}Cl + ^{154}Sm$, respectively. The time of flight (TOF) of a fission fragment was determined from the time "$T$" obtained from timing spectrum using the equation,

$$\mathrm{TOF} = T - T_{\mathrm{delay}} - T_{||}. \quad (1)$$

The total delay time $T_{delay}$ for a given detector, with respect to the beam pulse, was obtained by subtracting the calculated TOF of $^{35}Cl$ from the its peak in the timing spectrum. The TOF of fragments obtained after subtracting the delay gave a value of $V_{||}/V_{CN}$ slightly lower than unity, where $V_{||}$ is the velocity of the fissioning nucleus along the beam direction as obtained from the velocities of fission fragments [13] and

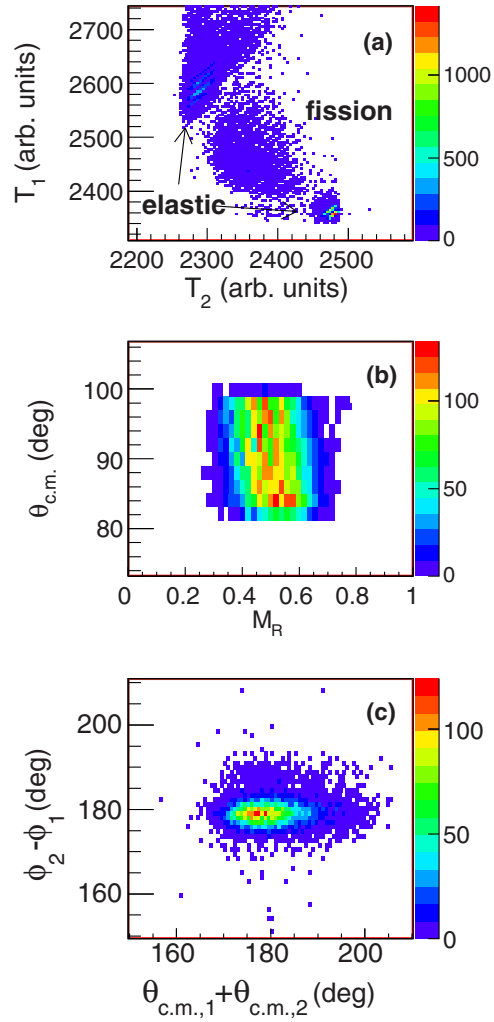


FIG. 1. (Color online) (a) Plot of timing spectrum for the $^{35}Cl + ^{144}Sm$ reaction at $E_{lab} = 156.1$ MeV (gated with $\theta_{c.m.} = 82^\circ - 99^\circ$). Fission fragments and elastically scattered particles are marked in the figure. (b) Plot of $\theta_{c.m.}$ vs mass ratio ($M_R = \frac{M_1}{M_1+M_2}$, where $M_1$ and $M_2$ are the mass numbers of coincident fission fragments). (c) Plot of "$\phi_2$-$\phi_1$" vs "$\theta_{c.m.,1} + \theta_{c.m.,2}$," subscripts 1 and 2 refer to the fragments detected in detectors 1 and 2, respectively.

$V_{CN}$ is the compound nucleus velocity calculated using beam energy. An additional parameter $T_{\parallel}(\leqslant 0.6\,\text{ns})$ was introduced to make $V_{\parallel}/V_{CN}$ unity. In the timing ($T_1$ vs $T_2$) spectrum, a gate was applied to select the fission fragments and reject the elastically scattered particles.

TOF values, obtained using Eq. (1), were used to calculate the laboratory velocities of the fission fragments. The effect of energy loss of the fragments in the target was negligible. For example, for the mass number 130, the effect of energy loss on the velocity was calculated to be about 1.3%. Hence, no correction was applied to the fragment velocities for energy loss in the target. Position calibration of the detector was carried out using the detector edges in the position spectrum. The $(X,Y)$ coordinates of the fragments were transformed into $(\theta,\phi)$. The laboratory values of $(\theta,\phi)$ and fragment velocities were transformed into the c.m. frame of reference using standard kinematic equations assuming full momentum transfer. c.m. velocities of fragments were used to calculate mass ratio ($M_R$) using equation,

$$M_R = \frac{V_{2,\text{c.m.}}}{V_{1,\text{c.m.}} + V_{2,\text{c.m.}}} = \frac{M_1}{M_{CN}}, \qquad (2)$$

where subscripts 1 and 2 refer to fragments registered in detector 1 and 2, respectively and "CN" refers to the compound nucleus.

## III. RESULTS AND DISCUSSIONS

A plot of $\theta_{\text{c.m.}}$ vs $M_R$ is shown in Fig. 1(b) for the $^{35}\text{Cl} + ^{144}\text{Sm}$ reaction at $E_{\text{lab}} = 156.1\,\text{MeV}$. Selection of the $\theta_{\text{c.m.}}$ range ensured the peaking of the $M_R$ distribution at ~0.5. However, for the $^{35}\text{Cl} + ^{154}\text{Sm}$ reaction at the lowest beam energy, the $M_R$ value was slightly lower (0.490) compared to 0.5. A plot of $\theta_{\text{c.m.},1} + \theta_{\text{c.m.},2}$ vs $\phi_2$-$\phi_1$ for the $^{35}\text{Cl} + ^{144}\text{Sm}$ reaction is shown in Fig. 1(c), which is centered around $(\theta_{\text{c.m.},1} + \theta_{\text{c.m.},2}) \sim 180^\circ$. The average values of the kinetic energies were in the range of $138 \pm 5\,\text{MeV}$ for both reaction systems, which is close to those calculated using Viola systematics [14], which was 138.9 and 136.6 MeV for the $^{179}\text{Au}(^{35}\text{Cl} + ^{144}\text{Sm})$ and $^{189}\text{Au}\,(^{35}\text{Cl} + ^{154}\text{Sm})$ systems, respectively. It should be mentioned here that the variation in total kinetic energy vs fragment mass did not show a perfect Gaussian behavior. However, its effect on the mass distribution is expected to be small (due to the linear dependence of fragment mass on velocity) and would be included in the mass resolution. An estimation of the mass resolution from the elastic peak was obtained to be around ~8.5 mass units.

Fission fragment mass distributions for the $^{35}\text{Cl} + ^{144}\text{Sm}$ and $^{35}\text{Cl} + ^{154}\text{Sm}$ reactions are shown in Figs. 2 and 3, respectively. The bin size in $M_R$ is 0.02, which correspond to 3.6 and 3.8 mass units for the $^{35}\text{Cl} + ^{144}\text{Sm}$ and $^{35}\text{Cl} + ^{154}\text{Sm}$ reactions, respectively. It can be seen from Figs. 2 and 3 that the gross behavior of the mass distribution appears to be symmetric for both $^{35}\text{Cl} + ^{144}\text{Sm}$ and $^{35}\text{Cl} + ^{154}\text{Sm}$ reactions. However, a single Gaussian is not sufficient to fit the experimental data, particularly for $^{35}\text{Cl} + ^{144}\text{Sm}$ reactions as seen from the $\chi^2$ values which are also given in the figure. Deviations from the single Gaussian fit are also shown in Figs. 2 and 3, below respective mass distributions. In order to ascertain

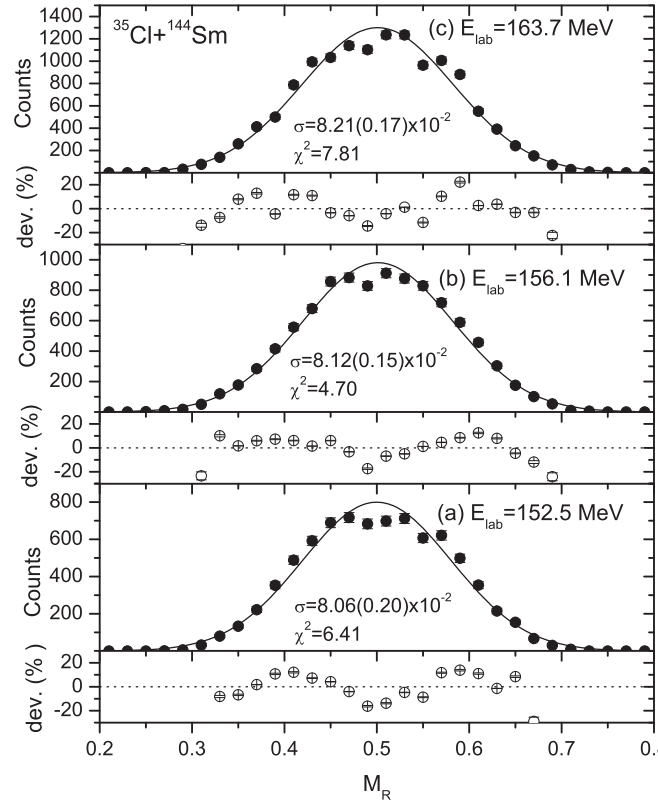


FIG. 2. Fission fragment mass distribution in the $^{35}\text{Cl} + ^{144}\text{Sm}$ reaction at (a) $E_{\text{lab}} = 152.5\,\text{MeV}$, (b) 156.1 MeV, and (c) 163.7 MeV. The filled symbols are experimental data, and the solid lines are fit to the data. The deviation of the experimental data from the fit is shown in the panel below the respective mass distribution (see text for details).

whether this deviation is related to multichance fission, the number of prefission neutrons ($\nu_{\text{pre}}$) and average excitation energies of the fissioning nucleus $\langle E_f^* \rangle$ were calculated using the code PACE2 [15]. Fusion $l$ distribution was calculated using the code CCFUS [16] and supplied as input for PACE2 calculations. For the coupled-channel CCFUS calculations, deformation data of the targets were taken from Refs. [17,18]. In PACE2 calculations, level density parameter was taken as $A/9\,\text{MeV}^{-1}$, $A$ being the compound nucleus mass number. Other parameters were kept as the default. Results of the calculations are given in Table I. As seen from this table, at a given beam energy, emission of prefission neutrons is more in the case of the $^{35}\text{Cl} + ^{154}\text{Sm}$ reaction compared to that in the $^{35}\text{Cl} + ^{144}\text{Sm}$ reaction due to the higher excitation energy and the $N/Z$ value of the compound nucleus, whereas deviation from a single Gaussian fit is more pronounced for the $^{35}\text{Cl} + ^{144}\text{Sm}$ reaction which has a lower excitation energy of the compound nucleus. Thus, deviations from the single Gaussian fit observed in the present study for the $^{35}\text{Cl} + ^{144}\text{Sm}$ reaction are most likely due to a contribution from an asymmetric component as predicted in calculations of Ref. [10] (ignoring the difference of one proton between $^{179}\text{Au}$ and $^{180}\text{Hg}$) due to the modification of the LDM potential-energy surface of the fissioning nucleus by single-particle effects. This is also consistent with the observation of a contribution from

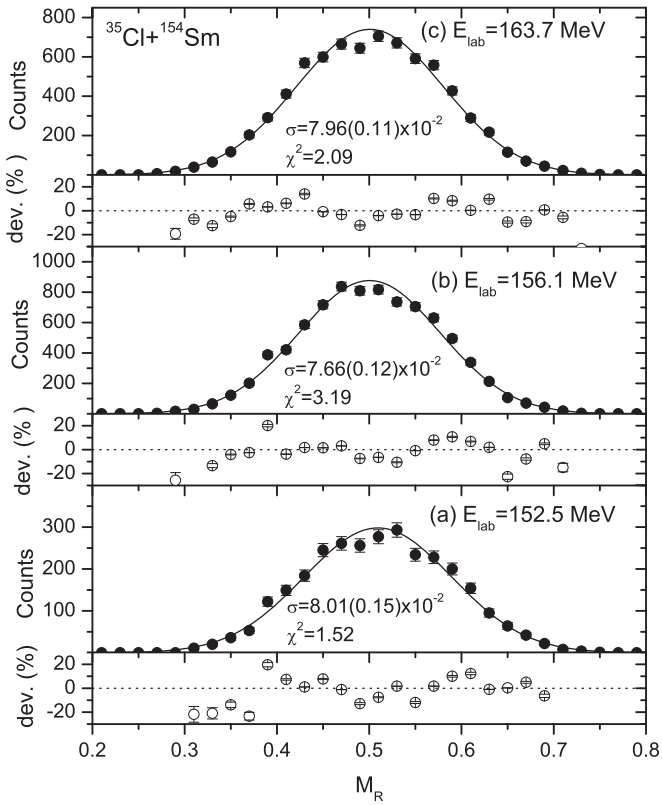


FIG. 3. Same as Fig. 2 but for the $^{35}$Cl + $^{154}$Sm reaction.

the asymmetric component in a recent measurement of mass distribution in the $^{40}$Ca + $^{142}$Nd reaction [12]. In calculations of Ref. [10], the asymmetric mass distribution has also been predicted for $^{188}$Hg, which is close to the compound nucleus for the $^{35}$Cl + $^{154}$Sm reaction. However, due to the larger excitation energy of the compound nucleus, the signature of asymmetric fission is weaker in the case of the $^{35}$Cl + $^{154}$Sm reaction. This leads to relatively smaller deviations from the single Gaussian fit for the $^{35}$Cl + $^{154}$Sm reaction arising from the higher chance fission for which the excitation energy of the fissioning nucleus would be lower. Although the deviations are observed at all the beam energies and for both reaction systems, a clear and systematic deviation as a function of mass was observed for the $^{35}$Cl + $^{144}$Sm reaction at the lowest beam energy, which can be used to obtain an estimate of the light and heavy fragment peaks of the asymmetric component. Maximum deviation occurs around $M_R \sim 0.41$ and $\sim$0.59 which correspond to fragment masses of about $\sim$73 and $\sim$176. Thus mass asymmetry observed in the present study is slightly on the lower side compared to that observed in the $\beta$-delayed fission of $^{180}$Tl [9]. However, the value observed in the present study is closer to that predicted in the calculations of Ref. [10].

The $\sigma$ values for the single Gaussian fits from the present study (given in Figs. 2 and 3) are comparable to those observed for the $^{40}$Ca + $^{142}$Nd reaction at similar excitation energies and much larger for those observed for the $^{12}$C + $^{182}$W reaction in Ref. [12]. Similar widths of the mass distribution in the $^{35}$Cl + $^{144,154}$Sm and $^{40}$Ca + $^{150}$Nd reactions suggest similar entrance channel dynamics, although not exactly the same. For example, an increase in the mass yield has been observed for $^{40}$Ca + $^{142}$Nd at larger mass asymmetry values. However, such an increase is not observed in the present study. In the study of fission fragment mass distribution in $^{48}$Ca + $^{144}$Sm reactions [8], an enhancement in fission fragment yield was observed corresponding to fragment neutron number $N = 50$, which corresponds to the symmetric fission for the $^{35}$Cl + $^{144}$Sm reaction. However, the presence of an asymmetric component in the mass distribution for the $^{35}$Cl + $^{144}$Sm reaction suggests that the potential-energy surface for the neutron deficient nuclei in the mass region around $\sim$180 is different from those for comparatively heavier fissioning nuclei. The effect of the potential-energy surface manifests in the fission fragment mass distribution as observed in $\beta$-delayed fission of $^{180}$Tl and the $^{40}$Ca + $^{142}$Nd reaction. A similar effect has also been observed in the reaction systems studied in the present paper. However, as discussed earlier a contribution from the asymmetric fission is more pronounced for the $^{35}$Cl + $^{144}$Sm reaction compared to that in the $^{35}$Cl + $^{154}$Sm reaction, possibly due to the lower excitation energy of the compound nucleus in the case of the $^{35}$Cl + $^{144}$Sm reaction. A comparison of the mass distribution at the lowest beam energy for the $^{35}$Cl + $^{144}$Sm reaction ($E^*_{CN} = 36.7$ MeV) with that for the $^{40}$Ca + $^{142}$Nd reaction ($E^*_{CN} = 33.6$ MeV) from Ref. [12] is shown in Fig. 4. Data from Ref. [12] have been normalized to

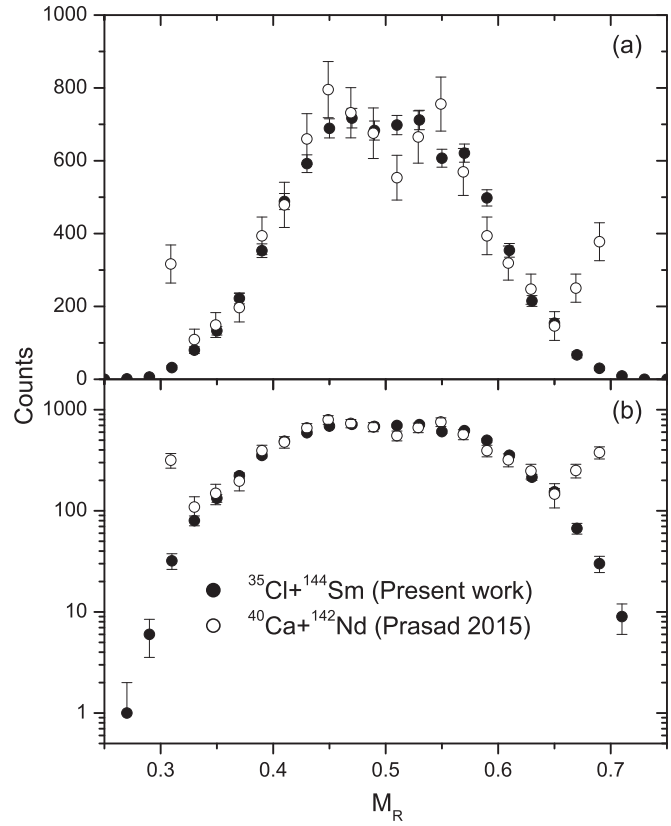


FIG. 4. (a) Comparison of fission fragment mass distribution in the $^{35}$Cl + $^{144}$Sm reaction with that in the $^{40}$Ca + $^{142}$Nd reaction from Prasad *et al.* [12]. Data from Ref. [12] have been normalized to the present data using the area in the $M_R$ range of 0.33−0.65. (b) is the same as (a) but for the logarithmic scale.

the present data using the area in the $M_R$ range of 0.33−0.65. The width of the mass distribution for $^{35}Cl + ^{154}Sm$ at the lowest beam energy is also similar, however it is not shown in the figure for the sake of clarity in the symmetric region. It can be seen from this figure that the mass distribution from the present paper and that from Ref. [12] are very similar but for the pronounced dip in the symmetric region observed for the $^{40}Ca + ^{142}Nd$ reaction. This suggests that the excitation energy in the present study is not low enough for the overall mass distribution to become asymmetric.

## IV. CONCLUSIONS

The measurement of mass distributions in $^{35}Cl + ^{144,154}Sm$ reactions was carried out at near-barrier energies. Although the mass distributions appear to be symmetric, they could not be fitted well with the single Gaussian function. The deviation from the single Gaussian fit was more pronounced for the $^{35}Cl + ^{144}Sm$ reaction as reflected in the large $\chi^2$ values. The deviation from a single Gaussian fit indicates the presence of an asymmetric component as observed in a recent measurement of fission fragment mass distribution in the $^{40}Ca + ^{142}Nd$ reaction [12]. The present result is also consistent with the theoretical prediction of Ref. [10], although the magnitude of the effect appears to be smaller. The flatness of the mass distribution in the symmetric region becomes clearly evident for $^{35}Cl + ^{144}Sm$ at the lowest beam energy. Also the mass distribution is very similar to that observed in the $^{40}Ca + ^{142}Nd$ reaction [12], although a clear dip in the symmetric region has not been observed, possibly due to the larger excitation energy in the present study.

## ACKNOWLEDGMENTS

We thank Dr. A. Goswami for his keen interest and many valuable suggestions during the course of this work. Thanks are due to the operating staff of the BARC-TIFR Pelletron-LINAC facility for a smooth run. We would like to thank Dr. D. C. Biswas for his help during the experiment.

[1] N. Bohr and J. A. Wheeler, Phys. Rev. **56**, 426 (1939).
[2] C. F. Tsang and J. B. Wilhelmy, Nucl. Phys. A **184**, 417 (1972).
[3] B. D. Wilkins, E. P. Steinberg, and R. R. Chasman, Phys. Rev. C **14**, 1832 (1976).
[4] V. M. Strutinsky, Nucl. Phys. A **95**, 420 (1967).
[5] J. Toke *et al.*, Nucl. Phys. A **440**, 327 (1985).
[6] A. Y. Chizhov *et al.*, Phys. Rev. C **67**, 011603(R) (2003).
[7] K. Nishio, H. Ikezoe, S. Mitsuoka, I. Nishinaka, Y. Nagame, Y. Watanabe, T. Ohtsuki, K. Hirose, and S. Hofmann, Phys. Rev. C **77**, 064607 (2008).
[8] G. N. Knyazheva *et al.*, Phys. Rev. C **75**, 064602 (2007).
[9] A. N. Andreyev *et al.*, Phys. Rev. Lett. **105**, 252502 (2010).
[10] P. Moller, J. Randrup, and A. J. Sierk, Phys. Rev. C **85**, 024306 (2012).
[11] A. V. Andreev, G. G. Adamian, and N. V. Antonenko, Phys. Rev. C **86**, 044315 (2012).
[12] E. Prasad *et al.*, Phys. Rev. C **91**, 064605 (2015).
[13] D. J. Hinde, M. Dasgupta, J. R. Leigh, J. C. Mein, C. R. Morton, J. O. Newton, and H. Timmers, Phys. Rev. C **53**, 1290 (1996).
[14] V. E. Viola, K. Kwiatkowski, and M. Walker, Phys. Rev. C **31**, 1550 (1985).
[15] A. Gavron, Phys. Rev. C **21**, 230 (1980).
[16] C. H. Dasso and S. Landowne, Comput. Phys. Commun. **46**, 187 (1987).
[17] S. Raman, C. W. Nestor, and P. Tikkanen, At. Data Nucl. Data Tables **78**, 1 (2001).
[18] T. Kibedi and R. H. Spear, At. Data Nucl. Data Tables **80**, 35 (2002).